A 13.56/402 MHz Autonomous Wireless Sensor Node with -18.2 dBm Sensitivity and Temperature Monitoring in 0.18 μm CMOS

Andre L.R. Mansano, Sumit Bagga and Wouter A. Serdijn
Section Bio-Electronics, Delft University of Technology, 2628 CD Delft, The Netherlands
E-mail: a.r.mansano@ieee.org, sumit.bagga@ieee.org, w.a.serdijn@tudelft.nl

***Abstract*—A multi-band autonomous wireless sensor node (AWSN) with temperature monitoring is designed in a standard 0.18 μm CMOS technology. The AWSN comprises a high efficiency energy harvester, a power management module, a temperature-to-time converter (TTC) and a passive 402-MHz MICS band OOK transmitter for backscattering transmission. The AWSN demonstrates a sensitivity of -18.2 dBm at 13.56 MHz. The energy harvester achieves an RF-to-DC power conversion efficiency (PCE) of 11.5 %. From 0 to 100 °C, the temperature conversion and temperature accuracy of the TTC are 1.5 μs/°C and 0.21 °C, respectively. The active area of the AWSN is 0.72 mm^2. It consumes 1.5 μW (RMS).**

I. Introduction

Until recently, power consumption was thought of as a hindrance towards the wider adoption and development of wireless sensor network (WSN) technology. Proven to be a sustainable energy source, the advancement of RF energy harvesting technologies has spurred considerable interest in reliable, cost-effective, low-power WSNs envisaged to monitor our environment. WSN nodes embedded with multiple functionalities are often deployed to monitor and control process variables like temperature, pressure, flow, level, etc.

Today's single-band/channel solutions for personal and body area networks rely on digital logic, ADCs, embedded memory for data management, and often require external elements (capacitors) for energy storage and power management [1-4]. This classical design methodology is relatively inflexible with respect to sensor accuracy and the required power budget tends to exceed what is permissible for autonomous operation. To overcome shortcomings of the classical design, this paper proposes an ultra low-power, general-purpose multi-band (MICS and ISM) autonomous wireless sensor node with temperature monitoring.

The paper is organized as follows. Section II presents the design of the AWSN. Measurement results are presented in Section III. Conclusions are drawn in Section IV.

II. Multi-Band Autonomous Wireless Sensor Node

As shown in Fig. 1, the AWSN comprises a passive high efficiency energy harvester, a power management module, a temperature-to-time converter and a 402 MHz (MICS band) OOK backscattering data transmitter. The multi-band approach is chosen to exploit the maximum permissible power transmission at 13.56 MHz, the wide bandwidth for data transmission at 402 MHz, thus providing simultaneous data communication and energy harvesting.

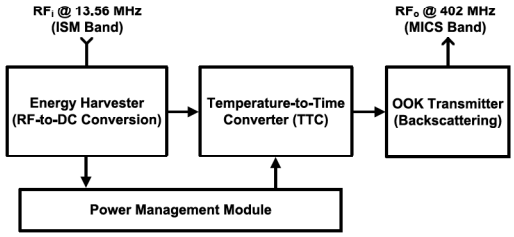

Fig. 1. Block diagram of the multi-band AWSN with temperature monitoring.

The theoretical model and analysis of the energy harvester is presented in [5]. The harvester comprises a passive voltage-boosting network (VBN) (Fig. 2(a)) and an orthogonally switching passive charge pump rectifier (OS-CPR) (Fig. 2(b)).

To adequately drive the OS-CPR, the VBN delivers large swing control (V_{b+} and V_{b-}) and energy signals (V_{r+} and V_{r-}). The resonant circuit of the VBN is modeled by the self-inductance of the antenna, L_A (9.5 μH), its series resistance, R_A (12 Ω) and capacitance $C_{V,T}$ (14 pF) (being the sum of the tuning and parasitic capacitances). An inductive choke L_C provides a DC short at the input terminals of the rectifier to ensure a zero DC offset error at the input of the OS-CPR. A single rectifier stage comprises PMOS transistors as voltage-controlled switches (M_1 and M_2) and capacitors for AC coupling (C_C) and energy storage (C_{R1} and C_{R2}). To reduce the unwanted flow-back current, capacitances C_{DC} and resistors R_{DC} set the optimum values of the gate voltages of M_1 and M_2. From a -18.2 dBm 13.56 MHz RF signal, a 5-stage OS-CPR sets the power supply voltage (V_{DC} = $V_{O,N}$) at 1.2 V.

Fig. 3 presents the all CMOS-based power management module. It includes a nanopower voltage reference, a linear voltage regulator and a low-voltage detector (LVD) with hysteresis (0.15 V). The reference produces a sub-1V, stable and temperature-independent voltage. With all the MOSFETs biased in weak inversion and the op-amp A_1 creating a virtual ground at $V_{\rm ref}$, the current through R_1 is PTAT. Proper selection of R_1, R_2 and N sets temperature-independent voltage $V_{\rm ref}$ at 0.54 V, which is derived by combining PTAT (V_{R2})

978-1-4799-5696-8/14/$31.00 ©2014 IEEE

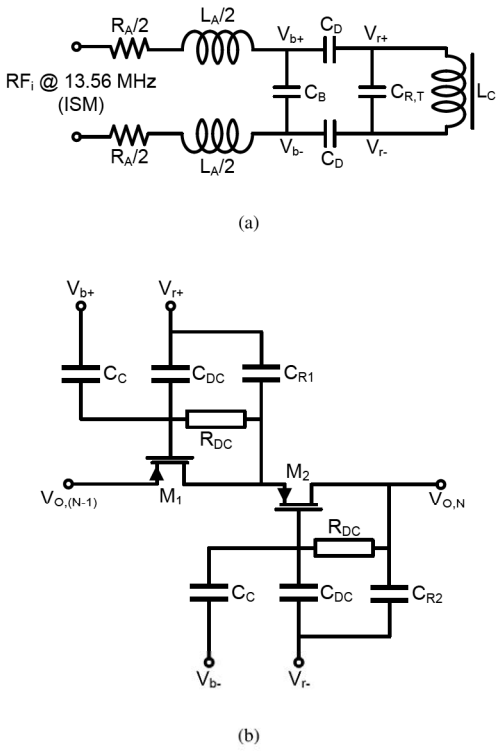

Fig. 2. The energy harvester comprises (a) voltage boosting network and (b) an orthogonally switching passive charge pump rectifier.

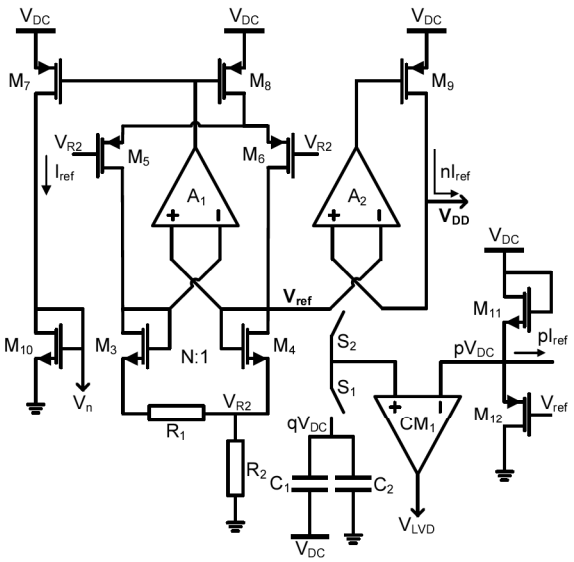

Fig. 3. Power management module of the AWSN.

and CTAT ($V_{\mathrm{gs},4}$) voltages. Current I_{ref} is steered into M_{10}, generating V_n used to generate nI_{ref}, mI_{ref} and pI_{ref}.

The linear regulator employs a unity gain buffer configuration to set the power supply (V_{DD}) of the AWSN at V_{ref}. Power supplies V_{DC} and V_{DD} are filtered using on-chip decoupling capacitors.

The low-voltage detector, which comprises switches S_1, S_2 and comparator CM_1, monitors the V_{DC} voltage level. During power-up V_{DC} initially is 0V and increases with time, until it reaches 1.2V. Also V_{ref} initially is 0V. The LVD operates as follows:

1) During power-up: S_1 is closed and the voltage divider formed by M_{11} and M_{12} sets $pV_{DC} < qV_{DC}$. To reduce static power consumption, qV_{DC} is generated from the capacitive divider formed by C_1 and C_2. Voltages qV_{DC} and pV_{DC} are compared by CM_1 and as long as the latter is smaller, the output voltage of the LVD (V_{LVD}) equals V_{DC}.
2) Steady-state: S_1 opens, S_2 closes and V_{ref} is connected to the input of CM_1. Once pV_{DC} equals V_{ref} (i.e. V_{DC} settles to 0.96 V), V_{LVD} goes from V_{DC} to 0 V, thereby enabling the temperature-to-time converter (TTC).

The TTC and the 402 MHz (MICS band) OOK transmitter are shown in Fig. 4. Derived from the circuit design presented in [6], the temperature-to-time encoded clock signal is generated by steering a weighted PTAT current (mI_{ref}) into an integrating capacitor (C_T). The slope of the resulting ramp-like analog waveform is compared to two voltage references, V_1=0.35 V for the rising and V_2=0.15 V for the falling edge transitions. The resulting output square wave signal of the TTC with a time period T_{TTC} is defined as

$$T_{TTC} = \frac{C_T \Delta V}{mI_{ref}}, \tag{1}$$

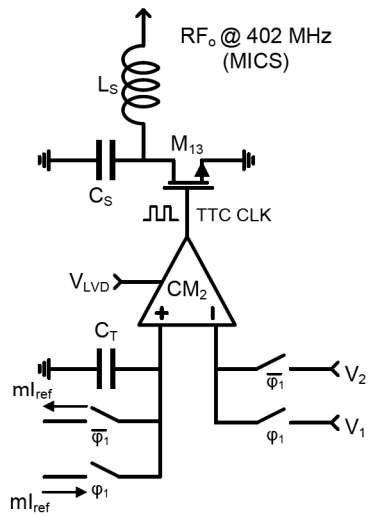

Fig. 4. Temperature-to-time converter and the 402 MHz (MICS band) OOK transmitter.

where $m = 2$, $\Delta V = V_1 - V_2$. A backscattering return link is formed at 402 MHz when the TTC clock signal drives/switches transistor M_{13}, thereby modulating the signal power.

III. Measurement Results

The AWSN is mounted on a double-sided, copper-clad FR-4 laminate substrate with a high quality factor coil (antenna) etched on the back plate (see Fig. 5). The physical and electrical properties of the customized antenna coil are presented in Table I. The coil is modeled using ADS Momentum.

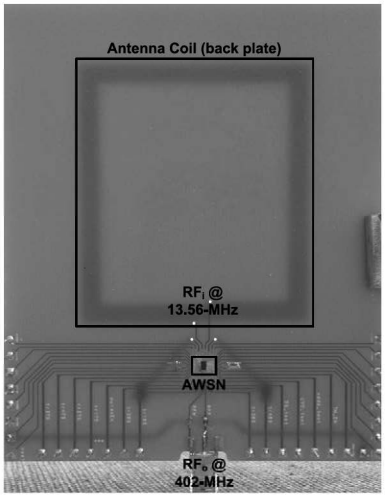

Fig. 5. The AWSN and the antenna coil on a 1/2 oz. 1.55 mm thick, double-sided FR-4 laminate substrate.

TABLE I
Physical and Electrical Properties of the Antenna Coil

Electrical	@13.56 MHz	Physical	1/2oz. 1.55mm
L_A (μH)	9.5	Outer dim. (mm^2)	56 x 50
R_A (Ω)	12	Inner dim. (mm^2)	48 x 42
C_A (pF)	2.4	Trace width (mm)	0.25
f_{SR} (MHz)	33	Trace space (mm)	0.25
Q-Factor	67	No. of turns	8

At 13.56 MHz, the measured real and imaginary impedance components of the antenna coil are 12.7 Ω and 0.81 kΩ, respectively (see Fig. 6). Simulation and measurement results show less than 5 $\%$ discrepancy.

The microphotograph of the AWSN fabricated in AMS 0.18 μm CMOS technology is shown in Fig. 7. The total and the active chip area are 2.64 mm^2 (1.2 x 2.2 mm^2) and 0.72 mm^2 (0.4 x 1.8 mm^2), respectively.

Superior to traditional topologies, the energy harvester operates over a large range of resistive loads (0.1 MΩ to 0.82 MΩ). As shown in Fig. 8, the maximum PCE is 11.5 $\%$ for a 0.82 MΩ load. Note that PCE equals the ratio of the electrical power delivered to the load and the incident electromagnetic power at the antenna.

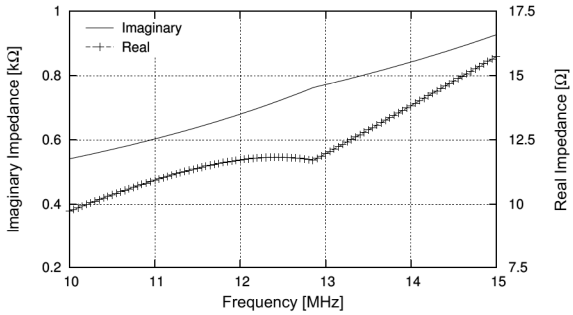

Fig. 6. Real and imaginary impedance of the antenna coil as a function of frequency.

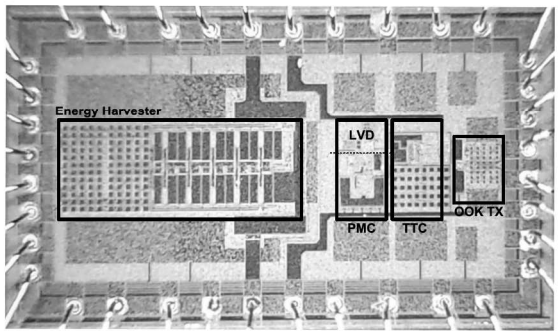

Fig. 7. Microphotograph of the AWSN in 0.18 μm CMOS.

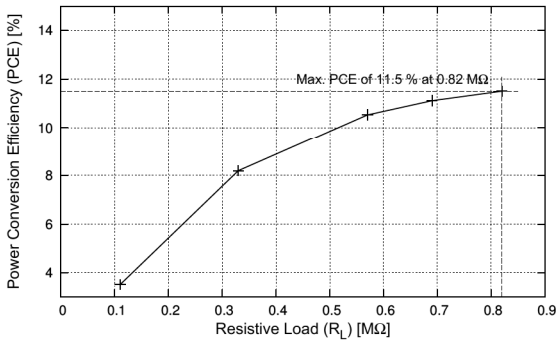

Fig. 8. PCE of the energy harvester as a function of resistive load.

The temperature conversion, jitter and temperature accuracy of the TTC are 1.5 μs/^{o}C, 320 ns and 0.21 ^{o}C, respectively, from 0 to 100 ^{o}C (see Fig. 9). The temperature accuracy ($TTC_{acc.}$) is calculated as the ratio of the jitter to temperature conversion and equals:

$$TTC_{acc.} = \left(\frac{320ns}{1.50\ \mu s/^o\mathrm{C}} \right) = 0.21\ ^o\mathrm{C} \qquad (2)$$

In compliance with MICS, the minimum clock period of the TTC is set to 20 μs. Fig. 10 shows the backscattering signal from the AWSN.

TABLE II
SUMMARY AND COMPARISON OF THE AWS WITH PREVIOUSLY PUBLISHED DESIGNS

Specifications	This Work	[1]	[2]	[3]	[4]
Frequency Bands (MHz)	13.56/402	2400	900/2100	13.56-2450	860-960
Sensitivity (dBm)	-18.2±1	-10.5	-19.7	-10.3	-6
Maximum PCE (%)	**11.5**	-	3	9	-
Conversion Accuracy (μs/°C)	1.5	-	-	-	-
Clock Jitter (ns)	320	-	-	-	-
Temperature Accuracy (°C)	**0.21**	0.37	-	0.34‡	0.20‡
Supply Voltage (V)	1.2	1.5	1.0	1.0	1.0§
Power Consumption (μW)	**1.5**	2.3	2.7†	2.7†	2.4†
Active area (mm^2)	0.72	0.7	1.055	0.95	1.1
Technology - CMOS	C-180	C-130	C-130	C-130	C-180

† Only sensor circuitry.
‡ Values estimated from ENOB.
§ Temperature sensor power supply.

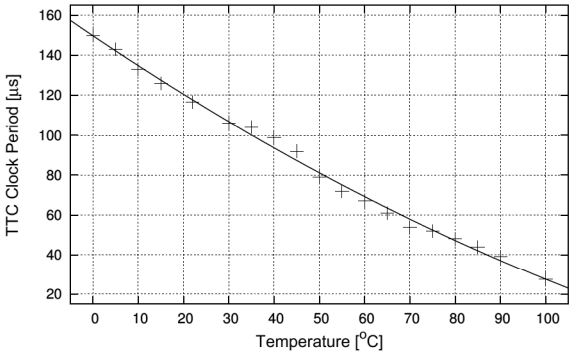

Fig. 9. Temperature conversion of the temperature-to-time converter. The least-squares polynomial regression shows a conversion accuracy of 1.5 $\mu s/^{o}C$.

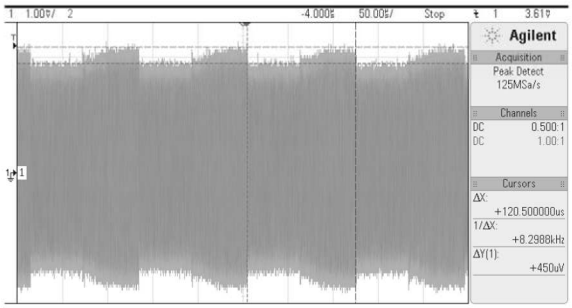

Fig. 10. Backscattered signal at 402 MHz (MICS band).

Table II compares the proposed AWSN to recently published designs. This work demonstrates superior design characteristics, such as high sensitivity, PCE and TTC accuracy with ultra-low power consumption. Moreover, the AWSN is both technology and frequency scalable.

IV. CONCLUSIONS

The proposed multi-band (13.56/402 MHz) autonomous wireless sensor node with temperature monitoring is fabricated in a standard 0.18 μm CMOS process. Scavenging a -18.2 dBm RF signal at 13.56 MHz, the energy harvester achieves a maximum power conversion efficiency of 11.5 %. From 0 to 100 °C, the temperature conversion and accuracy of the TTC are 1.5 μs/°C and 0.21 °C, respectively. The total RMS power consumption is 1.5 μW.

V. ACKNOWLEDGEMENTS

This work was supported by Delft University of Technology, the Netherlands and National Council for Scientific and Technological Development (CNPq), Brazil.

REFERENCES

[1] Y. Shih, T. Shen and B. Otis, "A 2.3 μW Wireless Intraocular Pressure/Temperature Monitor," *IEEE Journal of Solid State Circuits*, vol. 46, no. 11, pp. 2592-2601, 2011.

[2] H. Reinisch, S. Gruber, H. Unterassinger, M. Wiessflecker, G. Hofer, W. Pribyl and G. Holweg, "An Electro-Magnetic Energy Harvesting System With 190 nW Idle Mode Power Consumption for a BAW Based Wireless Sensor Node," *IEEE Journal of Solid State Circuits*, vol. 46, no. 7, pp. 1728-1741, 2011.

[3] H. Reinisch, M. Wiessflecker, S. Gruber, H. Unterassinger, G. Hofer, M. Klamminger, W. Pribyl and G. Holweg, "A Multifrequency Passive Sensing Tag With On-Chip Temperature Sensor and Off-Chip Sensor Interface Using EPC HF and UHF RFID Technology," *IEEE Journal of Solid State Circuits*, vol. 46, no. 12, pp. 3075-3088, 2011.

[4] J. Yin, J. Yi, M. K. Law, Y. Ling, M. C. Lee, K. P. Ng, B. Gao, H. C. Luong, A. Bermak, M. Chan, W.-H. Ki, C.-Y. Tsui and M. Yuen, "A System-on-Chip EPC Gen-2 Passive UHF RFID Tag With Embedded Temperature Sensor," *IEEE Journal of Solid State Circuits*, vol. 45, no. 11, 2010.

[5] A. Mansano, S. Bagga and W. Serdijn, "A IIigh Efficiency Orthogonally Switching Passive Charge Pump Rectifier for Energy Harvesters," *IEEE Transaction on Circuits and Systems I*, vol. 60, no. 7, pp. 1959-1966, 2013.

[6] Y. S. Lin, D. Sylvester and D. Blaauw "An Ultra Low Power 1 V, 220 nW Temperature Sensor for Passive Wireless Applications," *IEEE Custom Intergrated Circuits Conference*, pp.507-510, 2008.